Fabrication of Deterministic Nanostructure Assemblies with Sub-nanometer Spacing Using a Nanoimprinting Transfer Technique

Steven J. Barcelo,[†] Ansoon Kim,[†] Wei Wu,[‡] and Zhiyong Li[†,*]

[†]Hewlett-Packard Laboratories, 1501 Page Mill Road, Palo Alto, California 94304-1100, United States and [‡]Department of Electrical Engineering, University of Southern California, Los Angeles, California 90089, United States

ABSTRACT

Deterministic patterning or assembly of nanoparticles often requires complex processes that are not easily incorporated into system architectures of arbitrary design. We have developed a technique to fabricate deterministic nanoparticle assemblies using simple and inexpensive nanoimprinting equipment and procedures. First, a metal film is evaporated onto flexible polymer pillars made by nanoimprinting. The resulting metal caps on top of the pillars can be pulled into assemblies of arbitrary design by collapsing the pillars in a well-controlled manner. The nanoparticle assemblies are then transferred from the pillars onto a new substrate *via* nanoimprinting with the aid of either cold welding or chemical bonding. Using this technique, a variety of patterned nanoparticle assemblies of Au and Ag with a critical dimension less than 2 nm were fabricated and transferred to silicon-, glass-, and metal-coated substrates. Separating the nanostructure assembly from the final architecture removes significant design constraints from devices incorporating nanoparticle assemblies. The application of this process as a technique for generating surface-enhanced Raman spectroscopy substrates is presented.

KEYWORDS: nanoimprint · plasmonics · sensing · nanoscale devices · nanoparticle · SERS · nanofabrication

The fabrication of patterned metal nanoparticles is of intense interest for the growing field of plasmonics. The applications of localized surface plasmon resonances are diverse and powerful, including nanoscale optics,[1−3] chemical[4] and biological[5] sensing, photovoltaics,[6] and surface-enhanced Raman spectroscopy (SERS).[7] The specific arrangement of metal nanoparticles is particularly important for sensing techniques such as SERS, where many of the most successful designs capitalize on intense local electric fields generated by nanometer scale gaps between particles.[8,9] In some cases, enhancement strong enough for single-molecule spectroscopy has been reported.[10,11] Standard top-down and bottom-up approaches to fabricate arrays of particles with consistent gap size over a large area have been studied extensively, but have severe limitations. Nanoimprint lithography can be combined with e-beam lithography or other state of the art top-down approaches to produce nanoscale patterns on a large scale,[12] but direct patterning of nanometer scale gaps between particles proves challenging.[13,14] Conversely, bottom-up or self-assembly approaches allow for rapid fabrication[15] with good long-range order[16] and fine control of interparticle spacing,[8,17,18] but cannot be used to generate patterns of arbitrary design on a large scale. Even if these challenges can be overcome, fabrication of plasmonic nanoparticles is only the first step. To derive their true potential, it is necessary to seamlessly incorporate these structures into a more complex architecture, such as in optical[19] and photovoltaic devices[20,21] or lab-on-a-chip applications.[22,23] Here we will present a fabrication process that addresses both ends of this design challenge.

Some groups have used template-guided self-assembly techniques to generate nanoparticle assemblies with designable geometry,[24,25] but this approach requires modification of the final substrate, which makes incorporation of these structures into a general architecture difficult. Other groups have developed nanoscale pattern transfer techniques with resolution limited only by the initial patterning process, typically e-beam lithography,[26,27] and that can be used with nonplanar or extremely small substrates, such as optical fiber tips.[28] Previously, we demonstrated a technique combining top-down and self-assembly processes to generate arrays of

* Address correspondence to zhiyong.li@hp.com.

Received for review May 10, 2012 and accepted June 26, 2012.

Published online June 26, 2012
10.1021/nn3020807

metal particle groupings with arbitrary size, spacing, and geometry that can surpass the limits of even the most advanced lithography techniques.[29] However, the particle arrangements generated in these experiments sat on polymer pillars over a metal film, limiting their general application. In this paper we discuss a new process to overcome this constraint.

RESULTS AND DISCUSSION

The results presented here demonstrate a new technique to generate arrays of deterministic nanoparticle assemblies on a variety of substrates, creating the potential to incorporate plasmonic structures with arbitrary design and controllable interparticle spacing into a new platform separate from the original template. This new method is useful for SERS and other plasmonic applications, as it enables simple control over design variables such as the refractive index of the substrate and also enables easy integration of plasmonic structures into device architectures.

Metal Cap Transfer. The key steps of the metal nanoparticle fabrication and transfer process are illustrated in Figure 1, and the following is a brief overview of this process. First, an array of flexible polymer pillars is fabricated using a combination of e-beam lithography, reactive ion etching, and nanoimprint lithography according to a process described previously.[30] A thin layer of gold, silver, or other metal is then evaporated onto the pillar template, creating metal caps on top of the pillars over an underlying metal film. When these metal-capped pillars are exposed to a volatile liquid and subsequently dried, they collapse into predefined geometries due to microcapillary forces.[29,31] Once the pillar template is processed, a new substrate is prepared that is designed to bind to the metal caps more strongly to overcome the binding force between the metal caps and polymer pillars. The pillar template and substrate are then pressed together and placed back in the nanoimprinting tool. A pressure of 80 psi is applied to the bonded substrate stack to ensure conformal contact across the entire surface despite local surface height variations. After at least 12 h at room temperature, the pillar template and substrate are separated, transferring the metal caps to the new substrate. Shorter imprinting times were not tested but may be possible.

We will now discuss the process in more detail and its application to specific materials systems. The pillars fabricated in the first step consist of a UV-curable polymer that doubles as the nanoimprint resist.[32,33] The final nanoparticle diameter is defined by the original diameter of the polymer pillars, and the group symmetry after closing is defined by their initial spacing. When the nanopillars are exposed to a solution containing appropriate molecules and subsequently dried, the metal caps come into close proximity but are held apart by molecules adsorbed on the particle surface, forming nanometer-scale gaps. This is of particular interest for SERS applications, where nanoscale gaps are used to generate greatly enhanced local electric fields, referred to as "hot spots".[10,11] We have seen this effect using *trans*-1,2-bis(4-pyridyl)ethylene (BPE), which has two pyridine rings connected by a vinyl group. We previously demonstrated that the pyridyl nitrogen preferentially bonds to two adjacent gold particles, bridging the gap between them and simultaneously trapping the molecules in the SERS hot spot.[34] Other groups have achieved a similar effect in randomly aggregated nanoparticles using cucurbit[*n*]urils or DNA with trapped molecules to modify interparticle gap size by varying the molecular length.[8,17] Using this self-assembly approach, we are no longer limited by the resolution of the initial e-beam lithography pattern and can create arrays of particle assemblies with designable interparticle gaps down to the subnanometer scale. For example, the BPE molecule has a length of ~1 nm; therefore the gaps that we achieved using BPE as the ruler molecule were on the order of 1−2 nm, depending on whether a single molecule bridges the gap or molecules are adsorbed on both nanoparticles as they come into proximity. As shown below, the SERS performance of these substrates is consistent with this nanometer-scale gap size.

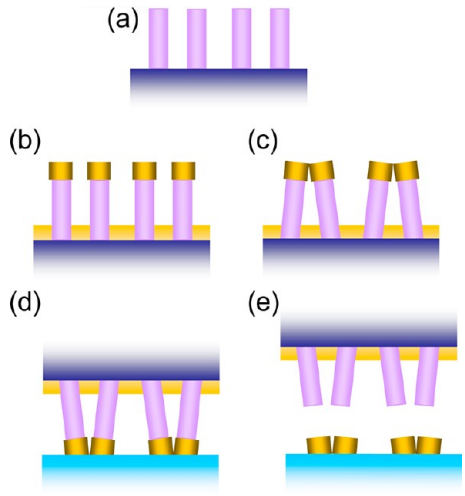

Figure 1. Nanoimprinting transfer technique, consisting of (a) fabrication of nanopillars using nanoimprint lithography; (b) deposition of metal on the nanopillar surface, forming the metal caps; (c) closing of pillars induced by microcapillary forces; (d) a second nanoimprinting process to bond the metal caps with the new substrate; and (e) transfer of the metal caps to the new substrate after separating the pillar template.

The full process flow outlined in Figure 1 is demonstrated for the transfer of Au caps to a new substrate in Figure 2a, c, and d. However, if particles with a larger spacing are desired, the pillar closing step can be skipped and the particles can be transferred directly, as shown in Figure 2b for Au caps transferred to an Au film surface. The initial particle spacing resolution is defined by the e-beam lithography step during the

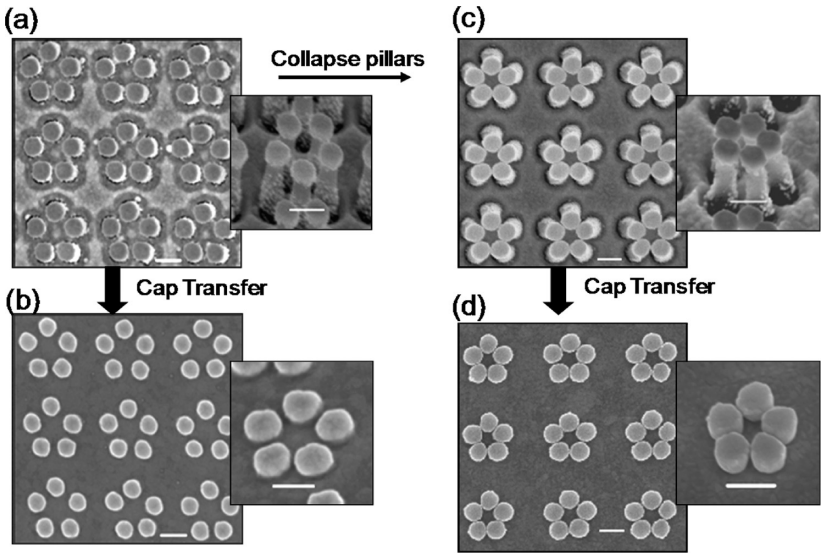

Figure 2. Representative SEM images showing the nanoimprinting transfer process to create pentagonal nanostructure assemblies. (a) Au caps on polymer pillars, (b) Au caps transferred to a new substrate without collapsing pillars, (c) Au caps on polymer pillars after collapse, and (d) Au caps transferred to a new substrate after collapsing pillars. All insets are taken at a 35° tilt view, and all scale bars are 200 nm.

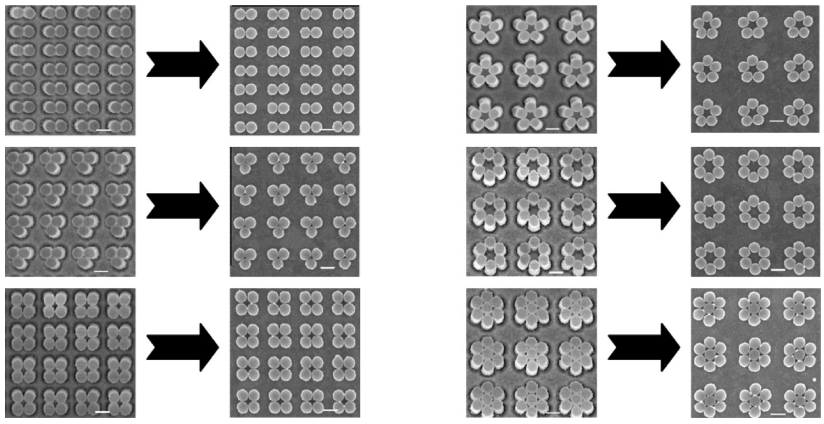

Figure 3. SEM images showing the versatility and deterministic control of nanoparticle assemblies by using a nanoimprint transfer process. Au caps on polymer pillars are arranged into a variety of patterns ranging from 2mers up to 7mers and faithfully transferred to an Au film. All scale bars are 200 nm.

fabrication of the nanoimprinting mold, while the closed nanoparticle spacing resolution is defined by molecules used to maintain the gap during the pillar closing step. Therefore this process yields fine control over particle spacing on both the micrometer and nanometer scale. Furthermore, the initial e-beam patterning step can be used to fabricate a variety of deterministic structures. As an example, the transfer of Au nanoparticle assemblies with various geometries ranging from 2mers up to 7mers to an Au-coated Si substrate is shown in Figure 3.

Techniques to Transfer to a Variety of Substrates. The results from two methods to generate the metal–substrate binding force are shown in Figure 4, along with a demonstration of the process for four different material systems. The first method relies on the strong bond formed when two like metals are pressed together, referred to as cold welding when no added heat is used.[35] While low-pressure cold welding between clean metal surfaces under ultrahigh vacuum is well known, it has also been observed in gold films under ambient conditions when at least one substrate is elastomeric.[36] Here we demonstrate the expansion of this technique to the transfer of patterned assemblies. In this application, a thin metal film is evaporated onto the new substrate, which is then pressed together with the metal-capped pillar template in a nanoimprinting tool. The flexible polymer pillars serve as an elastomeric support, ensuring conformal contact across the entire patterned area.

The second method consists of coating the new substrate with a self-assembled monolayer of molecules with exposed thiol functional groups, which binds strongly to most metals.[27,37] The other end of the molecule is terminated by a trichlorosilane headgroup, which bonds well to exposed hydroxyl groups

(−OH) on the substrate, forming a monolayer under appropriate conditions.[38,39] The self-assembly process was performed using a vapor phase molecular assembling method as previously reported.[40] The required hydroxyl groups can be formed on most oxides or substrates with a surface oxide layer either by a brief oxygen plasma treatment or a dip in piranha solution consisting of a 3:1 ratio of H_2SO_4 and H_2O_2.

These two methods are used to demonstrate the application of the nanoimprinting transfer technique to four different material combinations in Figure 4: Au particles on an Au film, Au particles on glass, Au particles on Si, and Ag particles on Si. Faithful transfer was achieved for >95% of all nanoparticle assemblies for all of the systems studied.

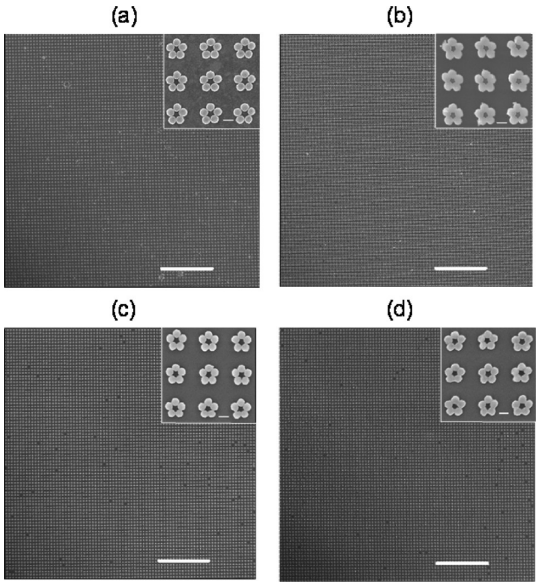

Figure 4. Representative SEM images showing large-scale cap transfer in four different material combinations. (a) Au caps transferred onto a 70 nm Au film on a Si substrate. (b) Au caps transferred to a glass substrate coated with a monolayer of thiol-terminated molecules. This sample was coated with 5 nm Al for imaging. (c) Au and (d) Ag caps transferred to a Si substrate coated with a monolayer of thiol-terminated molecules. The scale bars are 10 μm in the large field view images, and inset scale bars are 200 nm.

SERS Performance of Transferred Metal Caps. To demonstrate the potential of this process for generating SERS substrates in an arbitrary environment, we fabricated SERS substrates using two methods, outlined in Figure 5. Identical pillar templates were used in both cases, consisting of 130 nm diameter pillars arranged in a variety of geometries, from 2mers up to 7mers, and capped with 70 nm Au. The first pillar template was soaked in 1 mM BPE in ethanol, while the second was soaked in pure ethanol, each for 10 min, and then removed and allowed to air-dry, causing the pillars to collapse. The metal caps from both templates were then transferred to thiol-coated quartz substrates, and the second substrate was further soaked in 1 mM BPE in ethanol solution for another 10 min. All samples were rinsed in ethanol after exposure to BPE to remove physisorbed molecules.

SERS measurements for a variety of nanoparticle arrangements are shown in Figure 6. For a valid comparison across all geometries, the measured Raman peak intensity values were normalized by the particle density, which varied significantly from substrate to substrate based on the spacing between particle groupings and the number of particles per group. If we consider each point of contact between particles to be a potential hot spot, this is equivalent to normalizing the signal by the density of hot spots for all cases except for the 7mers. Since the 7mer arrangement already shows the lowest Raman peak intensity, accounting for potential additional hot spots in this geometry would not substantially change the presented results.

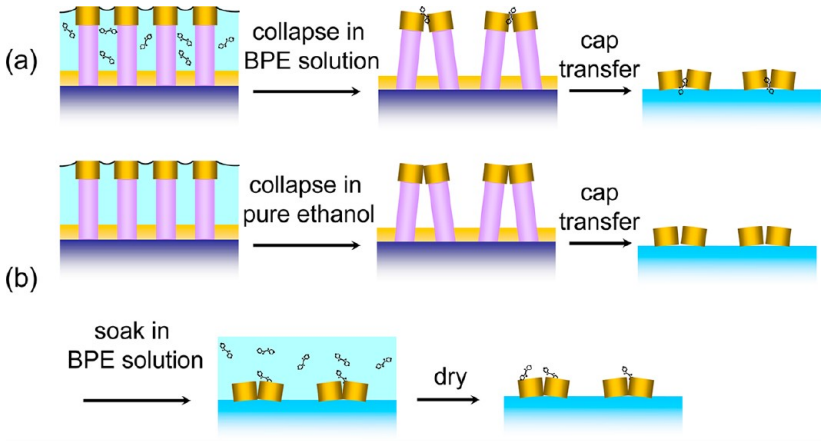

Figure 5. Depiction of two schemes for taking SERS measurements from Au particle groupings on quartz substrates. In the first scheme (a) the pillars were soaked in 1 mM BPE solution in ethanol. The substrate was dried in air, causing the pillars to collapse, and the metal caps were transferred to a quartz substrate with trapped BPE molecules. In the second scheme (b) the pillars were collapsed in pure ethanol. After the Au caps were transferred to a quartz substrate, they were soaked in 1 mM BPE solution in ethanol for 10 min and allowed to air-dry.

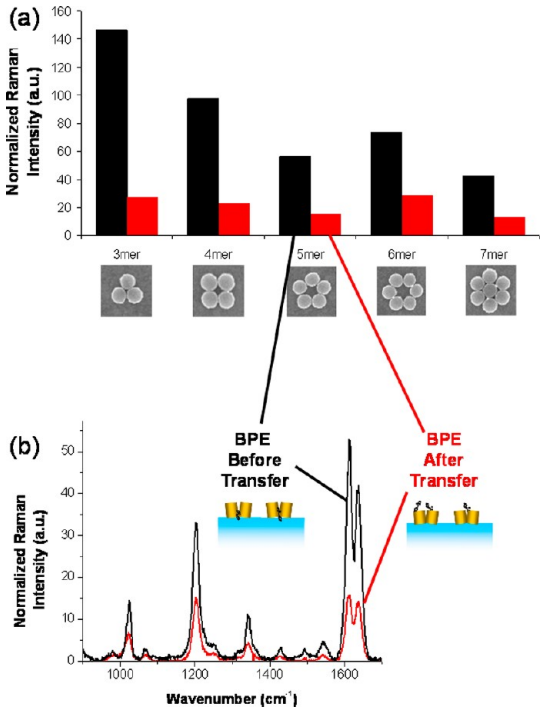

Figure 6. (a) Normalized Raman peak intensity at 1600 cm^{-1} for Au nanoparticles on quartz in a variety of arrangements. Black bars are for nanoparticles with trapped BPE before transfer, while red bars are for nanoparticles exposed to BPE after transfer. (b) SERS signal from transferred Au caps arranged as 5mers and exposed to 1 mM BPE in ethanol. For the black curve, BPE was trapped in the caps during the pillar closing step. For the red curve, the pillars were closed using pure ethanol as a solvent and caps were transferred to a quartz substrate before exposure to the BPE solution.

A strong SERS signal is observed for both preparation techniques, but the signal from particles exposed to BPE during the finger closing process is typically about 3−5 times stronger. Since the length of a BPE molecule is around one nanometer, the gap between particles maintained by BPE is below the resolution limits of a typical scanning electron microscope (SEM), and there is no observable difference between the two sample preparation methods. The reduced signal from preclosed metal particles is consistent with previous studies confirming that exposing the nanofingers to a solution containing the analyte molecule leads to molecular trapping in the hot spots.[30,34]

A calculation of the enhancement factor (EF) described in a previous report[30] based on a conservative estimate of the number of BPE molecules trapped between the transferred nanoparticles yields values ranging from 3×10^8 to 2×10^9 for the different geometries. This is lower than the enhancement factor of 10^{11} previously observed for BPE molecules trapped in nanofingers,[29] but shows performance exceeding or on par with other studies on SERS performance of nanoparticle arrays.[9,25,41] Furthermore, recent reports have shown that an enhancement factor on the order of 10^7−10^8 is sufficient for single-molecule spectroscopy.[42,43] Assuming a similar number of molecules find their way into the hot spots in the metal particle assemblies exposed to BPE after transfer, the same EF calculation yields values ranging from 2 to 5×10^8 in this case.

There are a number of potential explanations for the observed reduction in enhancement factor after the particles are transferred to a new substrate. First, in most cases there is no longer an underlying gold film, which could serve to reflect the emitted Raman signal, so that a larger fraction of the total Raman signal is collected. Furthermore, the particles have now been introduced to a new environment with a different refractive index,[44] which can lead to a significant red shift of the plasmon resonance and therefore also the optimal excitation wavelength. These changes can also impact the relative SERS performance ranking of the particle geometries. While 5mers in the original nanofinger configuration were shown to have the strongest SERS response in a previous report,[29] 3mers showed a stronger response after being transferred to quartz surfaces. Even though further study is needed in order to understand the origin of such change, coupling of the nanoparticles with the substrate may play a major role in altering the plasmonic characteristics and the radiation path, affecting the observed SERS performance ranking.

The additional reduction in enhancement seen in the particles exposed to BPE after transfer also has a few possible explanations. The SERS hot spots of the preclosed particles may be less effective since no molecules were present during the initial pillar collapse to maintain the small gaps required for the strongest local electric field enhancement. In addition, fewer molecules are optimally located in the hot spots when the particles are exposed to an analyte solution after closing. Finally, we have previously reported evidence that the pyridine rings of BPE molecules preferentially bind to the gold particle surface, likely creating a bridge between neighboring Au particles. In addition to maintaining a small gap, this also serves to orient the majority of the BPE molecules along the local electric field vector in the hot spots. In the case where preclosed nanoparticles are exposed to BPE, the orientation of the molecules will be more random. The reduced signal is most likely a combination of these scenarios, with fewer molecules falling into weaker hot spots in suboptimal orientations. However, 10^8 is still a very large EF, and this second preparation method may be useful for applications where exposure to the analyte solution before cap transfer is impractical.

CONCLUSION

We have demonstrated a new technique for generating arrays of metal particles with designable geometry and nanometer scale spacing. With straightforward chemical modifications, these patterns can be transferred to a variety of substrates without significantly

altering their structure, making this a viable method for integrating plasmonic structures into devices. This can also be used as a technique to tune the environment and therefore the properties of plasmonic structures. For example, transferring plasmonic structures onto a substrate with high refractive index such as Si can lead to large changes in the plasmon resonance. The technique was demonstrated as a process to transfer SERS-active particles onto an arbitrary substrate. The fact that pretrapped molecules still show a strong signal indicates that the patterns are transferred precisely, as nanometer scale shifts can drastically reduce the effectiveness of SERS hot spots. This could be an effective way to transfer SERS-active particles to a waveguide or lab-on-a-chip substrates, leading to an integrated functional system.

EXPERIMENTAL METHODS

Pillar Mold Fabrication. Pillar molds were fabricated using a method described previously.[30] In summary, the initial mold is defined *via* e-beam lithography, followed by a series of reactive ion etching and nanoimprint lithography steps to generate high aspect ratio flexible polymer pillars on a Si substrate. The pillars used in these experiments had a typical height of 500−700 nm and diameter of 130−170 nm. Before metal deposition, the polymer template is exposed to a brief oxygen plasma treatment to improve the surface wettability, ensuring consistent pillar closing behavior.

Adhesion Layer Preparation. All substrates where diced into 1 in.^{2} squares and cleaned in piranha solution, consisting of a 3:1 mixture of concentrated sulfuric acid and hydrogen peroxide, for at least 5 min. For bonding by cold welding, substrates were directly placed in a Leybold e-beam evaporator and 70 nm of the desired metal was deposited. For chemical bonding, the substrates were placed in a custom-built vapor phase molecular assembly machine and exposed to alternating flows of (3-mercaptopropyl)trimethoxysilane and water vapor.

SEM Measurements. All SEM images were taken in a FEI Sirion XL30 SFEG microscope with a 10 kV acceleration voltage using a through lens detector. Metal-coated polymer pillars and metal particles on conductive substrates were imaged without modification. Metal particles on nonconductive substrates such as quartz were coated with 5 nm Al before imaging.

SERS Measurements. In the basic procedure, samples were soaked in 1 mM BPE in ethanol for 10 min, allowed to air-dry, and subsequently rinsed with ethanol to removed physisorbed molecules. Specific modifications to this procedure are described in the main text. SERS measurements were performed using a Horiba JobinYvon T64000 upright confocal Raman microscope equipped with a liquid-nitrogen-cooled multichannel CCD detector. Samples were illuminated through a 100× (N.A. 0.9) objective with 784.6 nm laser light at 30 μW. The displayed spectra are the average of two measurements taken with a 3 s acquisition time. All chemicals were purchased from Sigma Aldrich without further modification.

Estimation of Enhancement Factor. The enhancement factor, EF, calculated here is defined as $EF = (I_{SERS}/N_{SERS})/(I_{bulk}/N_{bulk})$, where the Raman intensity is measured at the 1600 cm^{-1} peak in both cases. The bulk measurements were taken from 0.1 M BPE solution with a 100× objective with a large working distance to avoid contamination. With this setup, the laser illuminates a volume of approximately 125 μm^3, so that $N_{bulk} = 125\ \mu m^3 \times 0.1\ M \times N_{avogadro} = 7.53 \times 10^9$ molecules. To calculate N_{SERS}, we assume that the molecules within the 1 nm^3 volume between two nearly touching nanospheres experience the strongest enhancement and, therefore, contribute to the majority of the SERS signal. Assuming a close-packed monolayer of BPE molecules with a size of 3 Å × 6 Å × 10 Å each, there are approximately five molecules per hot spot. We can then estimate N_{SERS} on the basis of the particle density for a given geometry and the number of hot spots per particle. For example, for a 2mer there is one hot spot for every two particles, but for the 3mer, 4mer, and 5mer structures there is one hot spot per particle.

Conflict of Interest: The authors declare no competing financial interest.

Acknowledgment. This work is partially supported by DARPA. We also acknowledge F. S. Ou, M. Hu, and X. Li for their contribution to the development of the fabrication process.

REFERENCES AND NOTES

1. Barnes, W. L.; Dereux, A.; Ebbesen, T. W. Surface Plasmon Subwavelength Optics. *Nature* **2003**, *424*, 824–830.
2. Wang, W. H.; Yang, Q.; Fan, F. R.; Xu, H. X.; Wang, Z. L. Light Propagation in Curved Silver Nanowire Plasmonic Waveguides. *Nano Lett.* **2011**, *11*, 1603–1608.
3. Cai, W.; Brongersma, M. L. Nanoscale Optics: Plasmonics Gets Transformed. *Nat. Nanotechnol.* **2010**, *5*, 485–486.
4. Stewart, M. E.; Anderton, C. R.; Thompson, L. B.; Maria, J.; Gray, S. K.; Rogers, J. A.; Nuzzo, R. G. Nanostructured Plasmonic Sensors. *Chem. Rev.* **2008**, *108*, 494–521.
5. Haes, A. J.; Hall, W. P.; Chang, L.; Klein, W. L.; Van Duyne, R. P. A Localized Surface Plasmon Resonance Biosensor: First Steps Toward an Assay for Alzheimer's Disease. *Nano Lett.* **2004**, *4*, 1029–1034.
6. Atwater, H. A.; Polman, A. Plasmonics For Improved Photovoltaic Devices. *Nat. Mater.* **2010**, *9*, 205–213.
7. Moskovits, M. Surface-Enhanced Spectroscopy. *Rev. Mod. Phys.* **1985**, *57*, 783–826.
8. Taylor, R. W.; Lee, T.-C.; Scherman, O. A.; Esteban, R.; Aizpurua, J.; Huang, F. M.; Baumerg, J. J.; Mahajan, S. Precise Subnanometer Plasmonic Junctions for SERS within Gold Nanoparticle Assemblies Using Cucurbit[*n*]uril "Glue". *ACS Nano* **2011**, *5*, 3878–3887.
9. Wustholz, K. L.; Henry, A.-L.; McMahon, J. M.; Freeman, R. G.; Valley, N.; Piotti, M. E.; Natan, M. J.; Schatz, G. C.; Van Duyne, R. P. Structure-Activity Relationships in Gold Nanoparticle Dimers and Trimers for Surface-Enhanced Raman Spectroscopy. *J. Am. Chem. Soc.* **2010**, *132*, 10903–10910.
10. Xu, H.; Aizpurua, J.; Kall, M.; Apell, P. Electromagnetic Contributions to Single-Molecule Sensitivity in Surface-Enhanced Raman Scattering. *Phys. Rev. E* **2000**, *62*, 4318–4324.
11. Campden, J. P.; Dieringer, J. A.; Wang, Y. M.; Masiello, D. J.; Marks, L. D.; Schatz, G. C.; Van Duyne, R. P. Probing the Structure of Single-Molecule Surface-Enhanced Raman Scattering Hot Spots. *J. Am. Chem. Soc.* **2008**, *130*, 12616–12617.
12. Schmid, G.; Thompson, E.; Stacey, N.; Resnick, D. J.; Olynick, D. L.; Anderson, E. H. Template Fabrication for the 32 nm Node and Beyond. *Microelecton. Eng.* **2007**, *84*, 853–859.
13. Duan, H.; Hu, H.; Kumar, K.; Shen, Z.; Yang, J. K. W. Direct and Reliable Patterning of Plasmonic Nanostructures with Sub-10-nm Gaps. *ACS Nano* **2011**, *5*, 7593–7600.
14. Yang, X. M.; Xiao, S.; Wu, W.; Xu, Y.; Mountfield, K.; Rottmayer, R. Challenges in 1 Teradot/in.2 Dot Patterning Using Electron Beam Lithography for Bit-Patterned Media. *J. Vac. Sci. Technol. B* **2007**, *25*, 2202–2209.
15. Zhang, X.-Y.; Hu, A.; Zhang, T.; Lei, W.; Xue, X.-J.; Zhou, Y.; Duley, W. W. Self-Assembly of Large-Scale and Ultrathin Silver Nanoplate Films with Tunable Plasmon Resonance Properties. *ACS Nano* **2011**, *5*, 9082–9092.
16. Henzie, J.; Grunwald, M.; Widmer-Cooper., A.; Geissler, P. L.; Yang., P. Self-Assembly of Uniform Polyhedral Silver

Nanocrystals into Densest Packings and Exotic Superlattices. *Nat. Mater.* **2012**, *11*, 131–137.
17. Lim, D.-K.; Jeon, K.-S.; Kim, H. M.; Nam, J.-M.; Suh, Y. D. Nanogap-Engineerable Raman-Active Nanodumbbells for Single Molecule Detection. *Nat. Mater.* **2010**, *9*, 60–67.
18. Alivisatos, A. P.; Johnsson, K. P.; Peng, X.; Wilson, T. E.; Loweth, C. J.; Bruchez, M. P., Jr.; Schultz, P. G. Organization of `Nanocrystal Molecules' Using DNA. *Nature* **1996**, *382*, 609–611.
19. Ditlbacher, H.; Krenn, J. R.; Schider, G.; Leitner, A.; Aussenegg, F. R. Two-Dimensional Optics with Surface Plasmon Polartitons. *Appl. Phys. Lett.* **2002**, *81*, 1762–1764.
20. Pillai, S.; Catchpole, K. R.; Trupke, T.; Green, M. A. Surface Plasmon Enhanced Silicon Solar Cells. *J. Appl. Phys.* **2007**, *101*, 093105.
21. Yu, Z.; Raman, A.; Fan, S. Nanophotonic Light-Trapping Theory for Solar Cells. *Appl. Phys. A: Mater. Sci. Process.* **2011**, *105*, 329–339.
22. Diniz, L. O.; Margea, E., Jr.; Nunes, F. D.; Borges, B.-H. V. A Long-Range Surface Plasmon-Polariton Waveguide Ring Resonator As a Platform for (Bio)sensor Applications. *J. Opt.* **2011**, *13*, 115001–115007.
23. Chamanzar, M.; Soltani, M.; Momeni, B.; Yegnanarayanan, S.; Adibi, A. Hybrid Photonic Surface-Plasmon-Polariton Ring Resonators for Sensing Applications. *Appl. Phys. B: Laser Opt.* **2010**, *101*, 263–271.
24. Cui, Y; Bjork, M. T.; Liddle, J. A.; Sonnichsen, C.; Boussert, B.; Alivisatos, A. P. Integration of Colloidal Nanocrystals into Lithographically Patterned Devices. *Nano Lett.* **2004**, *4*, 1093–1098.
25. Yan, B.; Thubagere, A.; Premasiri, W. R.; Ziegler, L. D.; Dal Negro, L.; Reinhard, B. M. Engineered SERS Substrates with Multiscale Signal Enhancement: Nanoparticle Cluster Arrays. *ACS Nano* **2009**, *3*, 1190–1202.
26. Loo, Y.-L.; Willet, R. L.; Baldwin, K. W.; Rogers, J. A. Additive, Nanoscale Pattering of Metal Films with a Stamp and a Surface Chemistry Mediated Transfer Process: Applications in Plastic Electronics. *Appl. Phys. Lett.* **2002**, *81*, 562–564.
27. Loo, Y.-L.; Willett, R. L.; Baldwin, K. W.; Rogers, J. A. Interfacial Chemistries for Nanoscale Transfer Printing. *J. Am. Chem. Soc.* **2002**, *124*, 7654–7655.
28. Smythe, E. J.; Dickey, M. D.; Whitesides, G. M.; Capasso, F. A Technique to Transfer Metallic Nanoscale Patterns to Small and Non-Planar Surfaces. *ACS Nano* **2009**, *3*, 59–65.
29. Ou, F. S.; Hu, M.; Naumov, I.; Kim, A.; Wu, W.; Bratkovsky, A.; Li, X.; Williams, R. S.; Li, Z. Hot-Spot Engineering in Polygonal Nanofinger Assemblies for Surface Enhanced Raman Spectroscopy. *Nano Lett.* **2011**, *11*, 2538–2542.
30. Hu, M.; Ou, F. S.; Wu, W.; Naumov, I.; Li, X.; Bratkovsky, A.; Williams, R. S.; Li, Z. Gold Nanofingers for Molecule Trapping and Detection. *J. Am. Chem. Soc.* **2010**, *132*, 12820–12822.
31. Duan, H.; Berggren, K. K. Directed Self-Assembly at the 10 nm Scale by Using Capillary Force-Induced Nanocohesion. *Nano Lett.* **2010**, *10*, 3710–3716.
32. Ge, H.; Wu, W.; Li, Z.; Jung, G.-Y.; Olynick, D.; Chen, Y.; Liddle, J. A.; Wang, S.-Y.; Williams, R. S. Cross-linked Polymer Replica of a Nanoimprint Mold at 30 nm Half-Pitch. *Nano Lett.* **2005**, *5*, 179–182.
33. Wu, W.; Hu, M.; Ou, F. S.; Li, Z.; Williams, R. S. Cones Fabricated by 3D Nanoimprint Lithography for Highly Sensitive Surface Enhanced Raman Spectroscopy. *Nanotechnology* **2010**, *21*, 255502.
34. Kim, A.; Ou, F. S.; Ohlberg, D. A. A.; Hu, M.; Williams, R. S.; Li, Z. Study of Molecular Trapping Inside Gold Nanofinger Arrays on Surface-Enhanced Raman Substrates. *J. Am. Chem. Soc.* **2010**, *133*, 8234–8239.
35. Blackstock, J. J.; Li, Z.; Jung, G.-Y. Template Stripping Using Cold Welding. *J. Vac. Sci. Technol. A* **2004**, *22*, 602–605.
36. Ferguson, G. S.; Chaudhury, M. K.; Sigal, G. B.; Whitesides, G. M. Contact Adhesion of Thin Gold Films on Elastomeric Supports: Cold Welding Under Ambient Conditions. *Science* **1991**, *253*, 776–778.
37. Vos, J. G.; Forster, R. J.; Keyes, T. E. Formation and Characterization of Modified Surfaces. In *Interfacial Supramolecular Assemblies*; John Wiley & Sons: Chichester, UK, 2003; pp 89−94.
38. Bunker, B. C.; Carpick, R. W.; Assink, R. A.; Thomas, M. L.; Hankins, M. G.; Voigt, J. A.; Sipola, D.; de Boer, M. P.; Gulley, G. L. The Impact of Solution Agglomeration on the Deposition of Self-Assembled Monolayers. *Langmuir* **2000**, *16*, 7742–7751.
39. Ulman, A. Formation and Structure of Self-Assembled Monolayers. *Chem. Rev.* **1996**, *96*, 1533–1554.
40. Jung, G.-Y.; Li, Z.; Wu, W.; Chen, Y.; Olynick, D. L.; Wang, S.-Y.; Tong, W. M.; Williams, R. S. Vapor-Phase Self-Assembled Monolayer for Improved Mold Release in Nanoimprint Lithography. *Langmuir* **2005**, *21*, 1158–1161.
41. Li, W.; Camargo, P. H. C.; Lu, X.; Xia, Y. Dimers of Silver Nanospheres: Facile Synthesis and Their Use as Hot Spots for Surface-Enhanced Raman Scattering. *Nano Lett.* **2009**, *9*, 485–490.
42. Etchegoin, P. G.; Le Ru, E. C. A Perspective on Single Molecule SERS: Current Status and Future Challenges. *Phys. Chem. Chem. Phys.* **2008**, *10*, 6079–6089.
43. Le Ru, E. C.; Blakie, E.; Meyer, M.; Etchegoin, P. G. Surface Enhanced Raman Scattering (SERS) Enhancement Factors; a Comprehensive Study. *J. Phys. Chem. C* **2007**, *111*, 13794–13803.
44. Miller, M. M.; Lazarides, A. A. Sensitivity of Metal Nanoparticle Surface Plasmon Resonance to the Dielectric Environment. *J. Phys. Chem. B* **2005**, *109*, 21556–21565.